Hydraulic System Design and Vehicle Dynamic Modeling for the Development of a Tire Roller

Sang-Gyum Kim, Jung-Ha Kim, and Woon-Sung Lee

Abstract: In this paper, we describe a hydraulic system design and vehicle dynamic modeling for development of tire roller traction, an essential aspect in the system analysis of tire rollers. Generally, tire rollers are one of the most useful types of machines employed in road construction, technically applied to many construction fields. We also conceptualize a new hydraulic and driving system as well as define the motion equations for dynamic and hydraulic analysis. First, we design the hydraulic circuit of the steering control and driving machine system, which can be employed to advance the performance of the lateral control, creating a prototype of construction equipment. Second, we formulate the hydraulic steering system model and hydraulic driving system model through tire roller system development technology. Finally, we validate the acquired performance results in actual tire roller equipment using the data acquisition system. These results may perhaps facilitate the establishment of priorities and design strategies for incremental introduction of tire roller technology into the vehicle and construction field.

Keywords: Tire roller, driving system, steering system, hydraulic motor, hydraulic pump.

1. INTRODUCTION

For many years, scientists and engineers have envisioned creating new technology for construction equipment. Today, this technology has become increasingly significant due to the tremendous growth of industry technology, in particular the tire roller, which is commonly used in the final stages of road construction.

In some developed countries, tire rollers have been commercialized and their techniques have reached a very high level. However, domestic research and development in this field still leaves much to be desired even though the need for sophisticated construction equipment is keenly felt. Presently, most tire rollers are operated by a mechanical system, which has poor driving power and is difficult to control. This study proposes a hydraulic system that is easier to manage and has greater power than the typical mechanical system. We also attempt to analyze and design a mathematical model of the proposed system with the intention that, in developing tire rollers, the system analysis using mathematical modeling of the proposed system may bring certain advantages, such as shorter developing hours, cost-cutting and easier design, and verification of system analysis through test vehicles [1].

For efficient analysis and modeling for the proposed system, we first assumed that the tire roller system could be separated into two main parts: a steering system that consists of a hydraulic actuator, a flux valve and a steering linkage; and a driving system that consists of a diesel engine, a hydraulic pump, and a hydraulic motor. Second, the system analysis and modeling for each of the assumed systems were performed after consideration of the properties for component parts of the assumed systems [2, 3].

Finally, system analysis research using mathematical modeling for the suggested hydraulic system forms the basis of building up both the design and the system for the development of tire rollers and is also applicable to other equipment.

Manuscript received February 10, 2003; revised August 2, 2003; accepted September 10, 2003. Recommended by Editorial Board member Kyung Su Yi under the direction of Editor Keum-Shik Hong.

Sang-Gyum Kim is with the Graduate School of Automotive Engineering, Kookmin University, 861-1, Chungnung-dong, Sungbuk-gu, Seoul 136-702, Korea (e-mail: sanggyum@hotmail.com).

Jung-Ha Kim and Woon-Sung Lee are with the Graduate School of Automotive Engineering, Kookmin University, 861-1, Chungnung-dong, Sungbuk-gu, Seoul 136-702, Korea (e-mail: {jhkim, wslee}@kookmin.ac.kr).

2. SYSTEM CONFIGURATION

2.1. Analysis and modeling for the driving system

2.1.1 General modeling for the tire roller

To analyze the tire roller system, a vehicle model able to make an accurate estimate of possible phases in actual working conditions is required. This process of vehicle modeling, including the vehicle's dynamic behavior, such as starting, accelerating, steering, and

braking, should be performed with a close connection between the dynamic equations for the vehicle and the proposed hydraulic modeling. Therefore, it is important to perform modeling that can accurately reflect the actual motions of the tire roller. In general, the models for vehicle dynamic simulation varied with the purpose of their analysis and the data that we intended to obtain from them. For example, the models are as follows: a linear model having simple DOF (Degree Of Freedom), a nonlinear multibody dynamic model having more complicated DOF in using ADAMS (Automatic Dynamic Analysis of Mechanical System) or DADS (Dynamic Analysis and Design System), and a lumped parameter model according to data that contains system properties rather than component properties.

This paper introduces an established analysis method of a vehicle for development of a new vehicle model, which is applicable to tire rollers. Modeling and simulation results for a new vehicle model have been evaluated using data from the test vehicle. A vehicle simulation system applied to the developed tire roller is also used in the IO (Input and Output) system of the vehicle model and the vehicle's sub-system. Fig. 1 shows a FBD (Free Body Diagram) of the generalized tire roller model under static equilibrium by adding the inertial force at the center of gravity. Vectors in the figure indicate the force acting upon the vehicle when it starts on a slope [4, 5].

Fig. 1 is applied to the basic theory of the second law of Newton, and the fixed coordination of all the directions' external force sum is equal to the time variable rate of the momentum and is expressed as:

$$\sum F = \frac{d(mV)}{dt} = m\frac{dV}{dt}. \tag{1}$$

Furthermore, all moment sums of the external force are equal to the time variable rate of the moment of a momentum and are expressed as:

$$\sum M = \frac{dH}{dt}. \tag{2}$$

We will assume that the accurate performance of the hydraulic driving system is calculated from (3) by using the following assumptions:

(1) Chassis and steering linkage are rigid bodies.
(2) Symmetry with respect to a plane perpendicular to the rear axle and passing through its midpoint.
(3) Ground surface is planar and nondeformable.
(4) Eccentricities of the wheel are neglected since the loader has assumed a rigid body.
(5) Wheel reaction forces act at a single ground contact point between the tires and ground.
(6) Angular and vertical accelerations of the chassis are neglected.
(7) Aerodynamic forces are neglected.

$$\begin{aligned}(M + M_r)a_x &= \frac{W + W_r}{g} \times a_x \\ &= \frac{T_g}{r} - R_x - \mu W - W\sin\theta,\end{aligned} \tag{3}$$

where M: mass of the vehicle, M_r: equivalent mass of the rotating components, a_x: longitudinal acceleration, W: weight of the vehicle, W_r: dynamic weight, g: acceleration of gravity, T_g: torque generated on motor, R_x: rolling resistance forces, r: rolling radius of the tires, μ: coefficient of friction, θ: uphill grade.

2.1.2 Modeling of the driving system

The driving system of a tire roller consists of two pump motors. This application requires considerable horsepower for control purposes because of its high

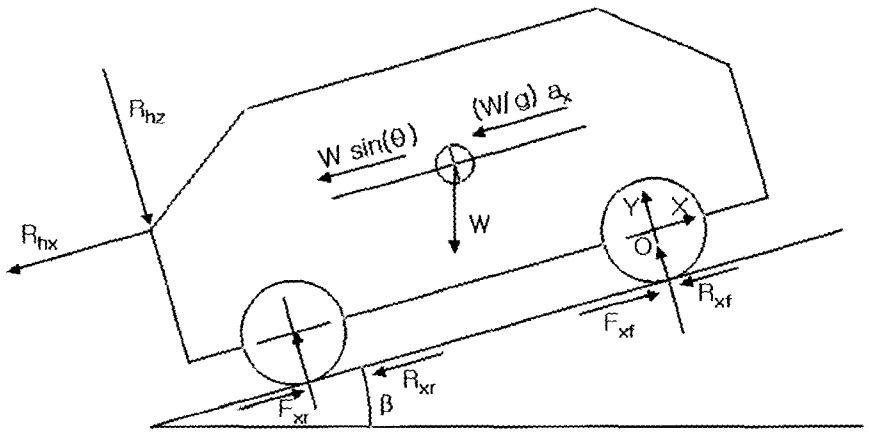

Fig. 1. F.B.D. of a generalized tire roller.

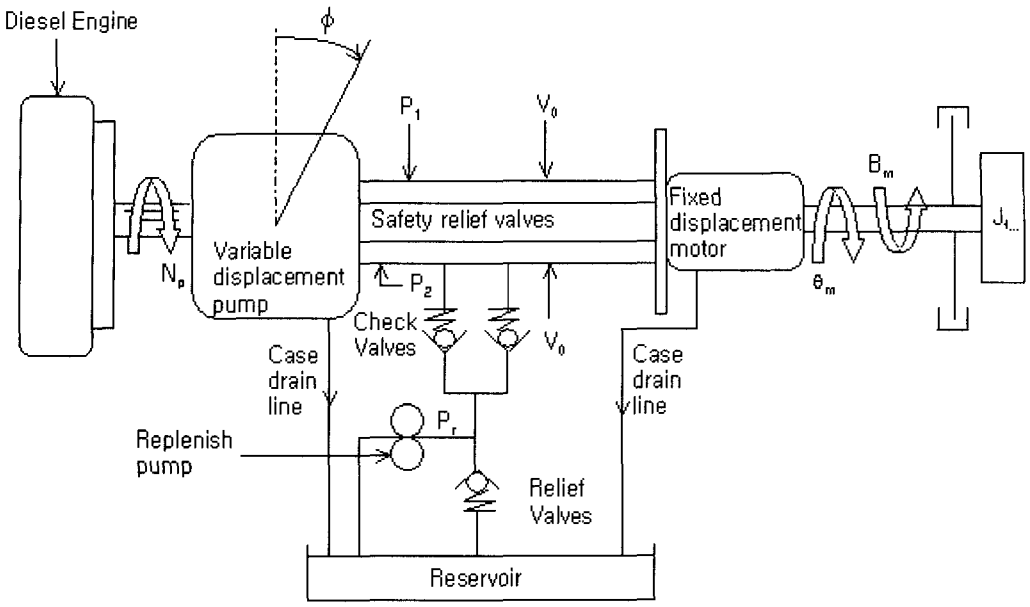

Fig. 2. Schematics of the driving controlled motor.

maximum operating efficiency, which can approach up to 90% in practice. Fig. 2 shows the schematic of a pump motor, which is often called a hydrostatic or hydraulic transmission [6, 7].

A variable displacement pump, which is driven by a constant speed power source and is capable of reversing the direction of flow, is directly connected to a fixed displacement hydraulic motor. Hence, the motor speed and direction of rotation may be controllable by varying the pump stroke. A replenishing supply is required to substitute leakage losses from each line and to maintain a minimum pressure in each line. During normal operation, the pressure in one line will be replenishing pressure, and the other line pressure will modulate to match the load. The two lines will switch functions if the load dictates a pressure reversal. It is possible for both line pressures to vary simultaneously if transients are rapid and load reversals occur. However, the research shall assume that only one line pressure varies at a time because this method uses more as a general rule. The load represents inertia of wheels on the tire roller. We assume that all pressure on the line is uniform, and ignore hydraulic line loss and pressure saturation, constant fluid density and temperature, constant chamber volumes in the pump and motor, replenishing pressure, pump speed, and leakage flows. Under these conditions, the continuity equation for the forward chamber can be written as [8]:

$$D_p N_p - C_{ip}(P_1 - P_r) - C_{ep}P_1 - C_{im}(P_1 - P_2) - C_{em}P_1 - D_m\frac{d\theta_m}{dt} = \frac{V_0}{\beta}\frac{dP_1}{dt}, \quad (4)$$

where D_p/D_m: volumetric displacement of pump and motor, N_p: velocity of pump (resume constant), C_{ip} /C_{ep}: internal / external leakage coefficient of pump, C_{im} /C_{em}: internal / external leakage coefficient of motor, P_1: pressure of front chamber, P_2: pressure of return chamber, P_r: replenishing pressure, V_o: average volume of forward chamber, β: fluid bulk modulus of system.

Pump displacement is calculated as:

$$D_p = k_p\phi, \quad (5)$$

where k_p: displacement gradient of pump control, ϕ: pump stroke angle.

Hydraulic motor torque is calculated as:

$$T = (P_1 - P_r)D_m. \quad (6)$$

Now, we can rewrite (4) and (6) of the second law of Newton.

$$T_m = (P_{m1} - P_{m2}) = J_t\frac{d^2\theta_m}{dt^2} + B_m\frac{d\theta_m}{dt} + \frac{\dot{\theta}_m}{|\dot{\theta}_m|}(P_{m1}+P_{m2})C_f D_m + T_L, \quad (7)$$

where J_t: moment of inertia, B_m: total viscous damping coefficient, $\dot{\theta}_m$: angular velocity of motor, C_f: internal motor friction coefficient, T_L: arbitrary load torque on motor.

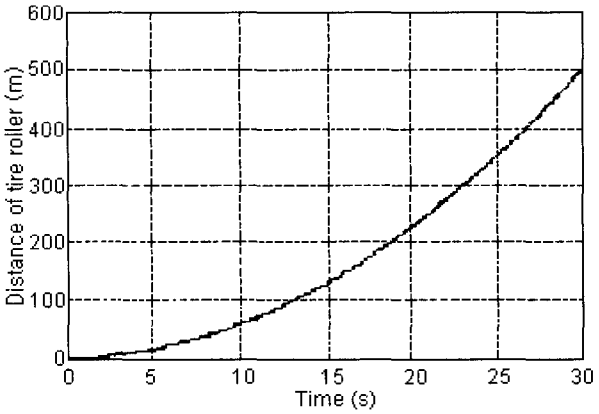

(a) Distance of tire roller (m).

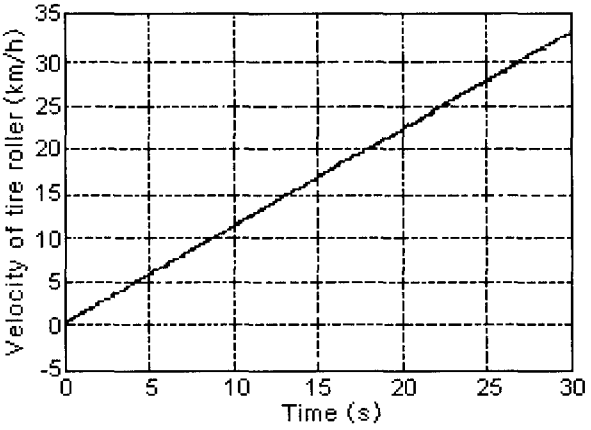

(b) Velocity of tire roller (km/h).

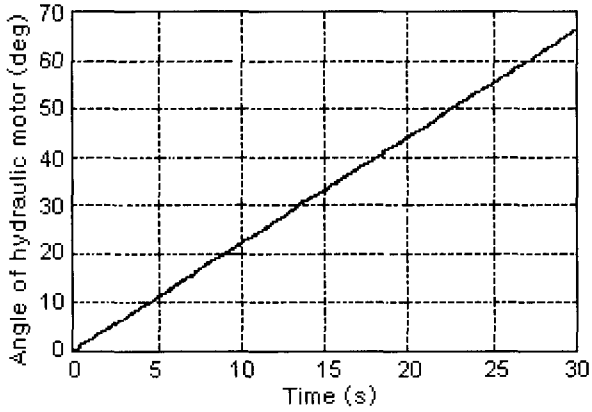

(c) Angle of hydraulic motor (degree).

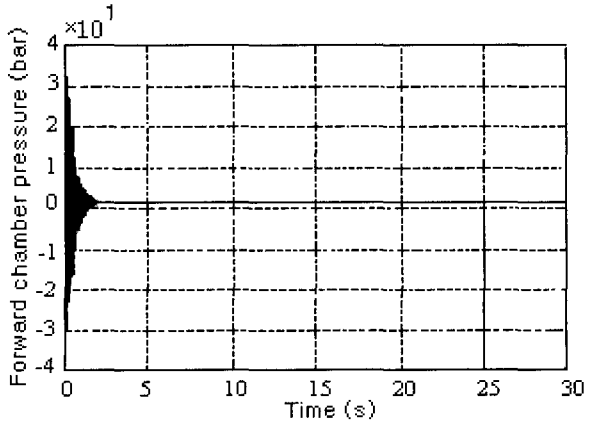

(d) Forward chamber pressure (bar).

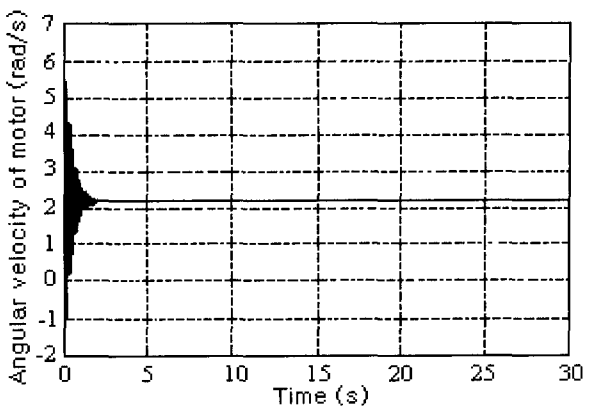

(e) Angular velocity of hydraulic motor (rad/s).

Fig. 3. Simulation results of driving system.

Therefore, in this study, the system modeling was performed through the previously mentioned equations, and the tire roller driving power was generated by the hydraulic motor rotation, which was measured as the acceleration sensor in the test vehicle. The vehicle velocity and acceleration were obtained by the velocity sensor on the transmission.

2.1.3 Mathematical representations and results

The driving system modeling of the vehicle is governed by combining the hydraulic system and tire roller model. The dynamic equation for the vehicle motion is:

$$X = \begin{bmatrix} d_x & v_x & \theta_m & \dot{\theta}_m & P_l \end{bmatrix} = \begin{bmatrix} x_1 & x_2 & x_3 & x_4 & x_5 \end{bmatrix}. \tag{8}$$

We can define five state variables from (9) to (13). Simulation results of the driving system modeling are shown in Fig. 3.

$$\dot{x}_1 = x_2, \tag{9}$$

$$\dot{x}_2 = \frac{g}{(w + w_r)}\left(\frac{(P_l - P_r)D_m}{r} - f_r w - w\sin\theta\right), \tag{10}$$

$$\dot{x}_3 = x_4, \tag{11}$$

$$\dot{x}_4 = \frac{(P_l - P_r)D_m - B_m\dfrac{d\theta_m}{dt}}{J_t} - \frac{\{(M + M_r)a_x + f_r W + w\sin\theta\}}{J_t} r, \tag{12}$$

$$\dot{x}_5 = \frac{\beta_e}{v_0}\left(D_p N_p - D_m \frac{d\theta_m}{dt}\right). \tag{13}$$

Fig. 3 (a) shows the tire roller moving distance according to time, which we can see increase consistently in vehicle distance. Fig. 3 (b) shows the

tire roller velocity according to time, which we know constantly accelerates in vehicle velocity. Fig. 3 (c) shows the angle from the hydraulic motor according to time. Fig. 3 (d) shows the forward chamber pressure variation according to time, in which we see the initial oscillation turn to a steady-state immediately. Fig. 3 (e) shows angular velocity of the hydraulic motor. These results should be in accord with actual driving experiments, and the results should be used for improving the design performance of the tire roller.

2.2. Analysis and modeling for the steering system

2.2.1 Hydraulic steering system modeling

In this research, the modeling of a hydraulic steering system has been designed relatively simply, and we assume that supply and drain pressures are constant. Each hydraulic actuator is connected to a two-rotary valve port, as shown in Fig. 4. The flow rate is calculated by using Bernoulli's equation. The hydraulic actuator on each side of the piston is applied to conserve the momentum equation. The steering system is controlled by the two actuators working in opposite directions [9].

The oil pressure in the actuator chamber is formulated as a first-order differential equation, which expresses the conservation of momentum.

$$\frac{V}{\beta_e}\dot{p} = Q - A\dot{y}, \tag{14}$$

where V: volume of chamber, β_e: effective bulk modulus, Q: flow delivery, $\dot{y}$: speed of piston, A: area of piston.

The translational force of an actuator is calculated by the difference between input and output pressures, and current position of the piston in the cylinder. These forces are used in the torque-force gain equations to produce equivalent torques at the body joints explained in the next section. The force generated by the actuator is calculated as:

$$f = p_1 A_1 - p_2 A_2 . \tag{15}$$

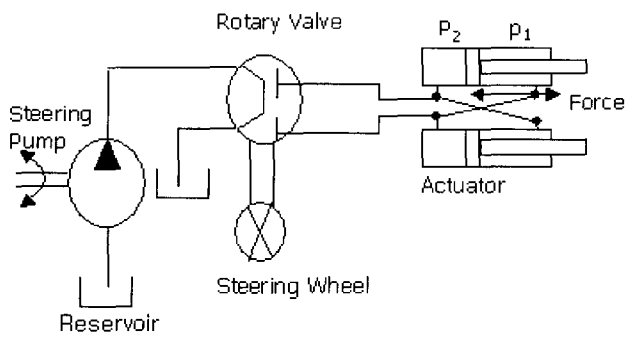

Fig. 4. Schematic of steering system.

2.2.2 Kinematics modeling of the steering system

Generally, the majority of tire rollers do not have suspension springs and dampers. Therefore, one end of a steering column is connected to the chassis with a revolution joint and the other end is attached to two hydraulic actuators, which control the steering angle. Forces applied for the hydraulic actuators are reformulated as equivalent torques acting on the steering because the steering is rotated according to the change of the actuator length. The equivalent steering torque is equal to the product of the actuator force and a torque-force of gain factor, which can be expressed using the principle of the virtual work theorem from this equation [10, 11].

$$\delta W = f\delta d - \tau\delta\theta = 0, \tag{16}$$

where δW : virtual work, f : actuation force, τ : equivalent torque acting on a joint, δd : virtual displacement of the actuator, $\delta\theta$: virtual rotation of the joint angle.

The torque-force gain factor, $g(\theta)$ is calculated as:

$$g(\theta) = \frac{\tau}{f} = \frac{\partial d}{\partial \theta} . \tag{17}$$

In Fig. 5, the center circle represents the steering column while h1 and h2 express a change in the length of the two actuators, which are controlled by the steering angle. From the two vector loops we obtained the following equations [10]:

$$h_1 = -s_3 + A_{2,1}s_{1,} \tag{18}$$

$$h_2 = -s_4 + A_{2,1}s_{2,} \tag{19}$$

where d1=||h1|| and d2=||h2|| are the relative length of the actuators, and $A_{2,1}$ is the relative rotational matrix based on the chassis, which is written as:

$$A_{2,1} = \begin{bmatrix} \cos(\theta) & -\sin(\theta) & 0 \\ \sin(\theta) & \cos(\theta) & 0 \\ 0 & 0 & 1 \end{bmatrix} . \tag{20}$$

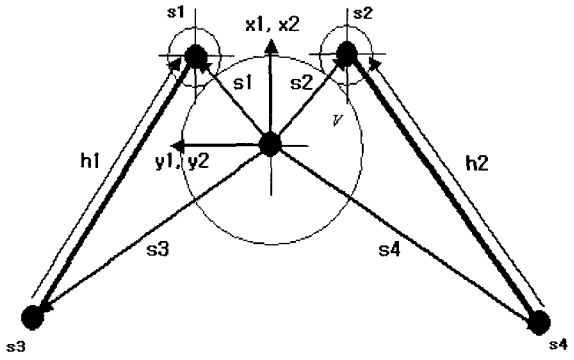

Fig. 5. Kinematics representation of the steering system.

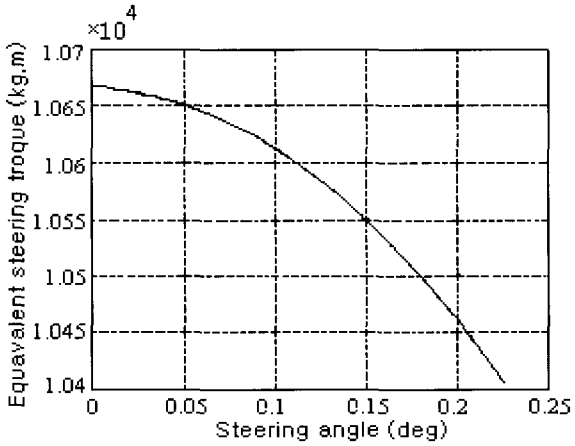

(a) Equivalent steering torque (kg·m).

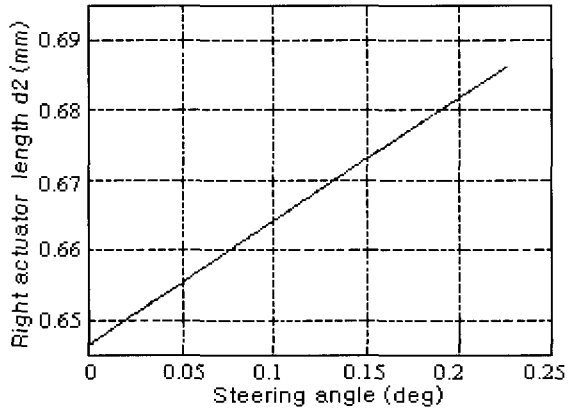

(a) Right actuator length displacement (mm).

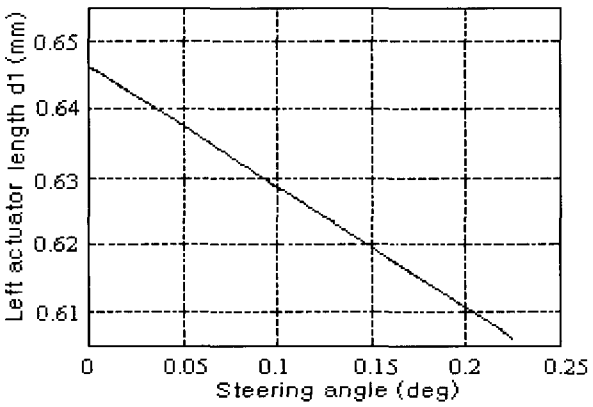

(c) Left actuator length displacement (mm).

Fig. 6. The actuator displacement and equivalent steering torque with the steering angle.

(17) is applied to the vector equation, which we obtained as:

$$g_i(\theta) = \frac{\partial}{\partial \theta}(d_i) = \frac{\partial}{\partial \theta}(\sqrt{h_i^T h_i}) = \frac{1}{d_i} h_i^T \frac{\partial h_i}{\partial \theta} = \frac{1}{d_i} h_i^T \frac{\partial A_{2,1}}{\partial \theta} s_i \,. \quad (21)$$

Thus, the total torque of the steering column can be expressed as the sum of the two actuator forces.

$$\tau = \frac{1}{d_i} h_1^T \frac{\partial A_{2,1}}{\partial \theta} s_1 f_1 + \frac{1}{d_2} h_2^T \frac{\partial A_{2,1}}{\partial \theta} s_2 f_2 \,. \quad (22)$$

Finally, each actuator velocity can be expressed relative to the rotational velocity of the steering column.

$$\dot{d}_1 = g_1 \dot{\theta}, \quad (23)$$

$$\dot{d}_2 = g_2 \dot{\theta}. \quad (24)$$

Now, we can calculate the change of the actuator length and equivalent steering torque according to the steering angle from (22) to (24).

Fig. 6 depicts the actuator displacement and equivalent steering torque according to the steering angle. Fig. 6 (a) shows the equivalent steering torque of the steering angle, and Figs. 6 (b) and (c) illustrate the actuator length displacement of the steering angle during the vehicle's right and left turning. From Figs. 6 (b) and (c), we can see the constant increase and decrease of the actuator length according to the steering angle.

3. EXPERIMENTAL DEVICE AND METHOD

3.1. Composition of the experimental device

The block diagram representation of the combined experiment system is shown in Fig. 7. A number of sensors used for the experiment produce the sensor signal. The encoder and acceleration sensor are used for the wheel's rotational and engine speed measurement, and the pressure sensor is used in the pipeline flow-mass pressure measurement. The steering angle is measured from the potentiometer according to flow-mass pressure. The combined signals are obtained from the data acquisition system and lab-view program [12, 13].

We show the dynamic performance index of the tire roller system in Table 1, and it is necessary to decide the system parameters by using the model in the design.

4. EXPERIMENTAL RESULTS AND INVESTIGATION

4.1 Experimental results of the driving system

Fig. 8 depicts the four conditions of the simulation and test results: motor RPM for vehicle by the time and pressure difference of the hydraulic motor inlet and outlet, which was obtained under plate angle variations of the plate pump through a computer

Table 1. Dynamic performance index of the tire roller.

Item	Index	Equation	Working on uphill	Working on flat	Driving on uphill	Driving on flat	Note
F (N)		$F = (W + W_r) * a / 9.8 + (\mu + \sin\theta) * W$	6433.83	1362.41	4557.30	1760.46	
T (N-m)		$T_{Total} = F * r$	3216.92	681.21	2278.65	880.23	
N (rpm)		$n = V / (2\pi * r)$	32	32	160	160	
Motor	T(N-m)	$T_{pump} = T_{Total} / 2$	1608.46	340.61	1139.33	440.12	
	n(rpm)	$n = V / (2\pi * r)$	32	32	160	160	
	Displacement (Cm^3 / rev)	$q = 2\pi * T / (P * \eta)$	458.34	97.06	324.66	125.42	
	Delivery(lpm)	$Delivery = q * n * 2 / \eta$	32.27	6.84	114.29	44.15	
Pump	Delivery(lpm)	$Delivery(Motor = Pump)$	32.27	6.84	114.29	44.15	
	Displacement (Cm^3 / rev)	$Displacement = Delivery / n$	14.67	3.11	51.95	20.07	
	Reference	$Motor\ and\ Pump\ Pressure = 250(bar),\ Engine\ Maximum\ Torque = 2200(rpm)$					
Engine power (kw)		$L = P * Q / (612 * \eta)$	14.65	3.11	51.88	20.04	
Note		−. $Working$: $Maximum\ Velocity = 6km / h$, $Accelerati\ on = 0.8333$, $Weight = 12000\ kg$, $Braking\ dis\tan ce = 0.7m$, $Braking\ time = 1.1(sec)$ −. $Driving$: $Maximum\ Velocity = 30km / h$, $Acceleration = 0.8333(uphill)$, $1.667(flat)$, $Weight = 8500kg$, $Braking\ dis\tan ce = 30m$, $Braking\ time = 8(sec)$ −. $Plate\ Angle = 25$, $Wheel$ Radius = 0.5m −. $Steering\ axle\ pressure = 100(bar)$ −. $Driving\ axle\ pressure = 250 - 300\ (bar)$ −. $Minimum\ Rotation\ Radius = 9m$ −. $Steering\ Angle$: $Left = 13^{\circ}$, $Right = 13^{\circ}$ −. $Cylinder\ Stroke$: $400(mm)$					

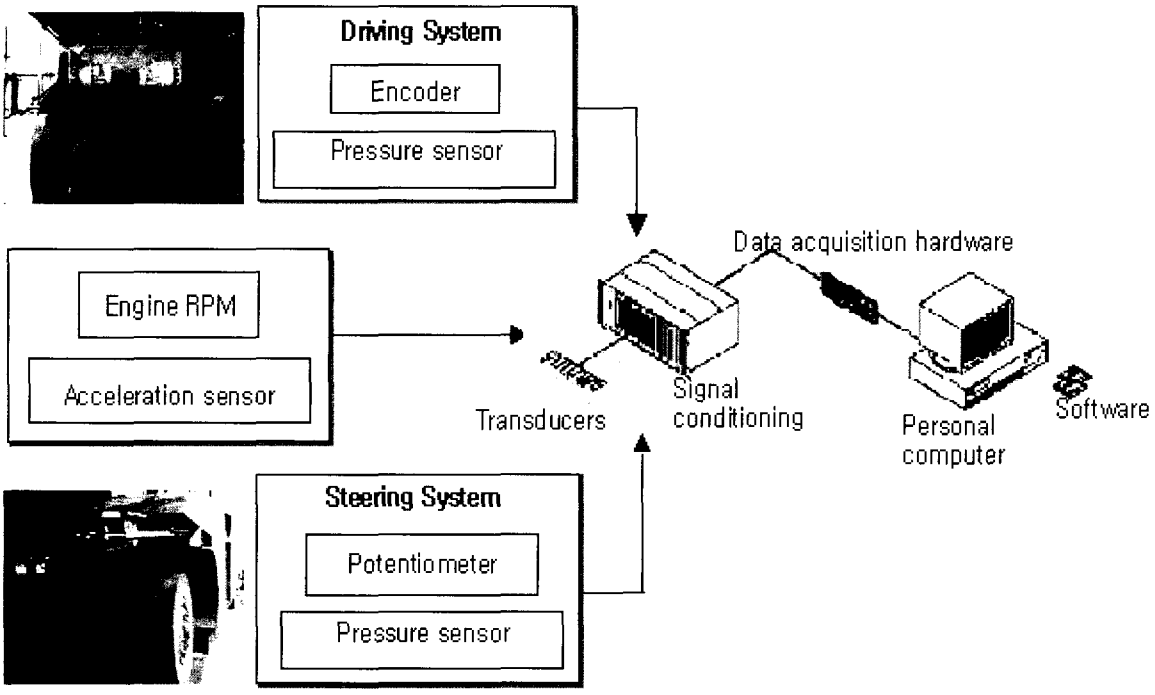

Fig. 7. Block diagram of the experimental measuring device.

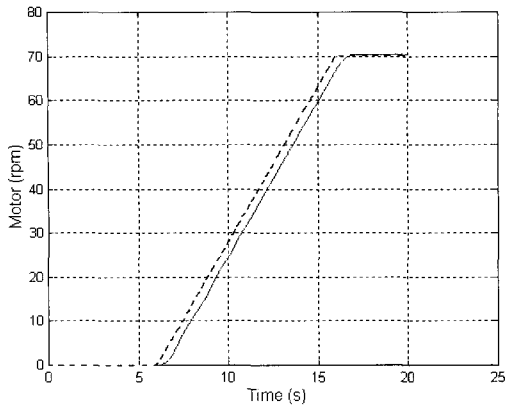

(a) Motor RPM.

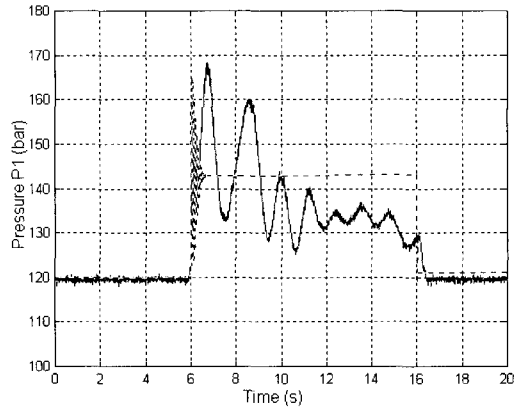

(b) Input pressure value.

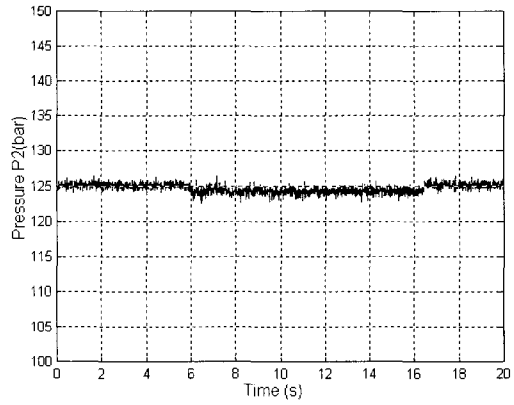

(c) Output pressure value.

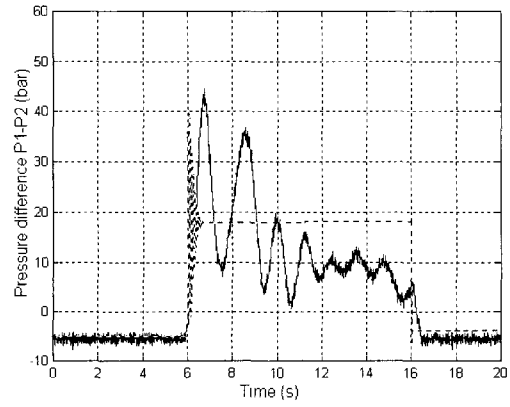

(d) Pressure difference.

Fig. 8. Driving system results.

simulation and the test vehicle, respectively. Each was performed with a ramp input signal given to a plate angle under the test condition that the tire roller is operated normally, keeping its engine RPM (1000 RPM) uniform. Moreover, simulation results are compared with the test vehicle results, as shown in Fig. 8.

In Fig. 8, we compare two lines: the dotted line expresses simulation results, and the hard line expresses the vehicle test results. Fig. 8 (a) shows the motor speed variation according to the plate angle, which is stabilized after a constant increase. Figs. 8 (b) and (c) show each of the pressure variations of the hydraulic line inlet and outlet. We know that the inlet pressure variation of the initial step dramatically rises once steady-state is maintained, while the outlet pressure variation displays very little variation. Fig. 8 (d) shows the pressure difference of the inlet and outlet.

From the simulation and driving test results, we can determine a difference between them, which is brought on by a simple modeling error and uncertainty of parameter tuning in the driving test. However, we know from looking at the overall system that the simulation and driving test results appear very similar to the trend.

4.2. Experimental results of the steering system

The steering system of the tire roller consists of the hydraulic actuator, rotary valve, and steering pump, which display the full motion of the vehicle. The steering angle is determined by the revolution angle that the steering handle and valve spool release. The simulation was performed by the commercial EASY5 program package, and its results were verified through vehicle testing.

The simulation and vehicle test results are detailed in Fig. 9. The simulation and vehicle test experiment was performed with a step signal given to the steering system in two conditions: releasing the time of the valve spool (0.01 seconds) and constant engine RPM (1000 RPM).

In Fig. 9, we compare the two lines: the dotted line expresses the simulation results, and the hard line expresses the vehicle test results. Fig. 9 (a) shows the cylinder displacement according to the step input signal, which stabilizes after constant increase. Figs. 9 (b) and (c) show each of the pressure variations of the inlet and outlet in the hydraulic actuator according to the step input signal. The inlet and outlet pressures of the initial step are a smaller fluctuant and steady-state maintenance. Fig. 9 (d) indicates the pressure difference of the inlet and outlet.

Results of the steering sine wave input are shown in Fig. 10, and are equal to Fig. 9 during test conditions.

From the results of the simulation and driving test,

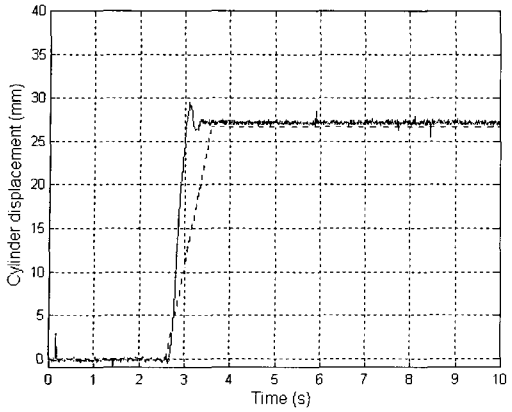

(a) Cylinder displacement.

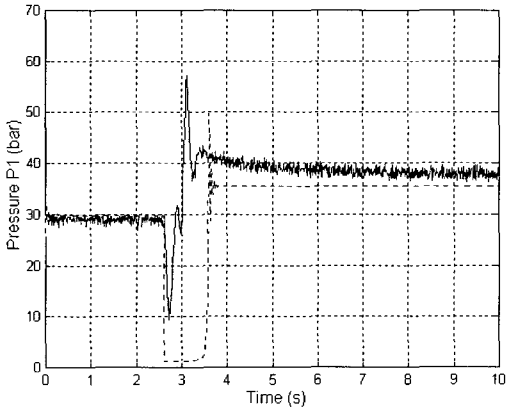

(b) Input pressure value.

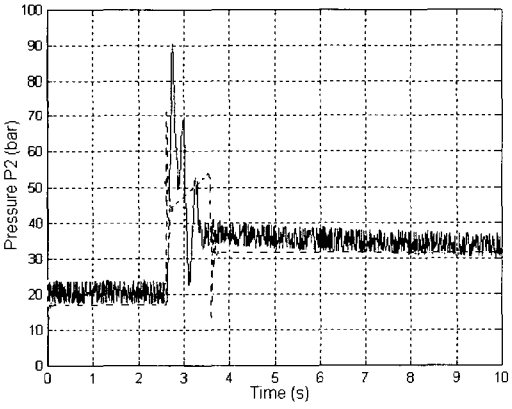

(c) Output pressure value.

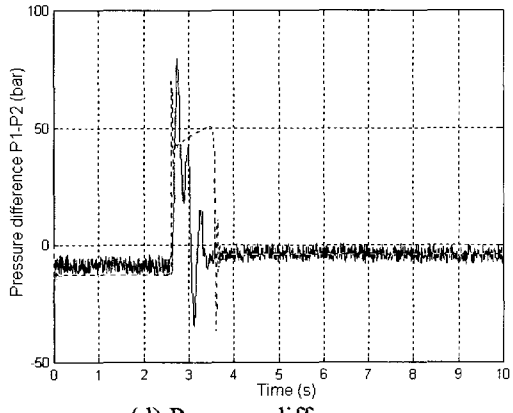

(d) Pressure difference.

Fig. 9. Steering system results (step input).

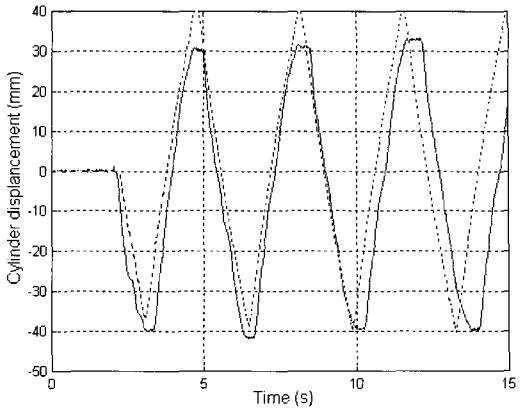

(a) Cylinder displacement.

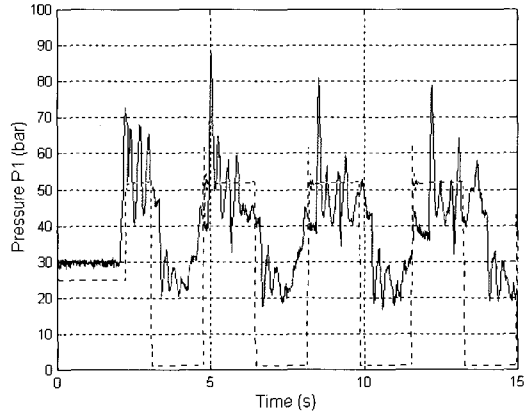

(b) Input pressure value.

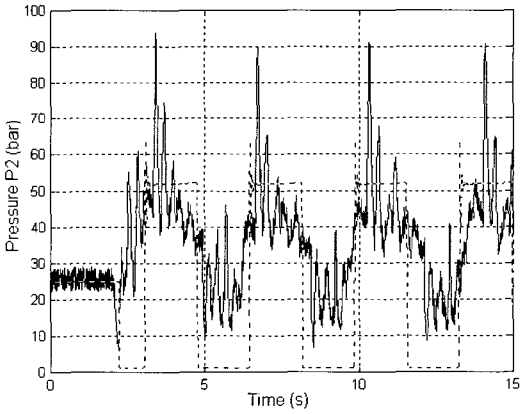

(c) Output pressure value.

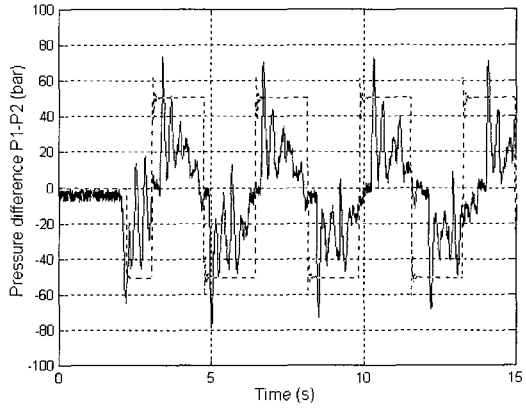

(d) Pressure difference.

Fig. 10. Steering system results (sine wave input).

we can observe a difference between the step input and sine input results, which are brought on considering only a few important parameters as an input value.

However, we can also recognize from the step and sine input according to steering that the results of the simulation and driving test appear very similar to the trend.

We can further realize that hydraulic change of the hydraulic line can be estimated and it is almost even during initial pressure.

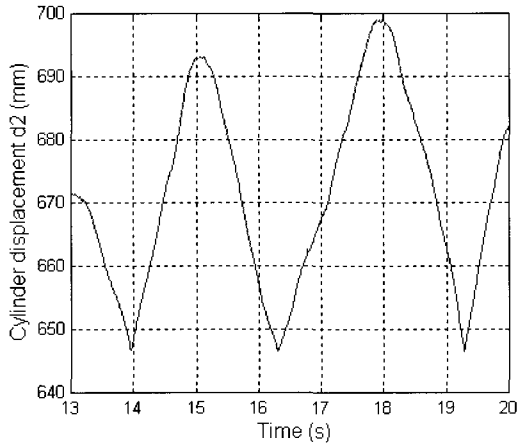

(a) Steering angle response.

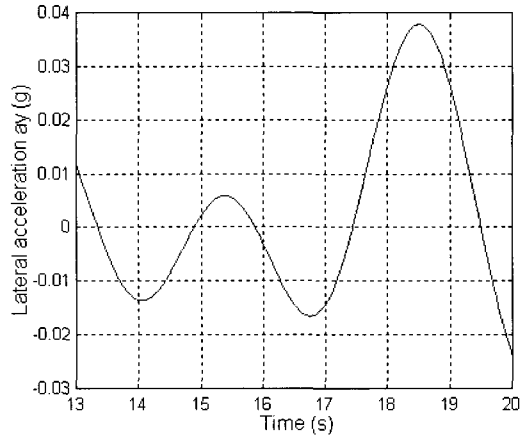

(b) Lateral acceleration response.

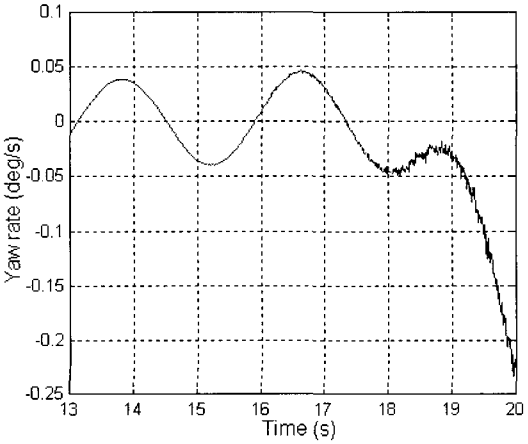

(c) Yaw rate response.

Fig. 11. Vehicle behavior (sine wave steering input).

4.3. Vehicle behavior

The vehicle behavior of the steering sine wave input is shown in Fig. 11. Fig. 11 (a) shows the cylinder displacement of the steering input, which wave is the same as the sine wave form. Figs. 11 (b) and (c) show the lateral acceleration and yaw rate response. We know that the vehicle behavior is similar to the sine wave steering input.

5. CONCLUSIONS

We have described in this paper a new analysis and design for a mathematical model for the tire roller operated by a hydraulic system, including the driving system model and the steering system model. Simulation tools used to develop and evaluate such a system have also been presented. Simulation and vehicle test experiments were performed with an input data signal given to the systems for each of these models. We also examined simulation results and the vehicle test results. The summary of the results is as follows:

(1) In the simulation and vehicle test for the driving system, we calculated the parameters for the hydraulic tire roller: vehicle moving distance, velocity and angular velocity of the driving motor, and the pressure difference at the motor outlet. The results are compared and analyzed by the simulation and vehicle test experiment.

(2) For the simulation and vehicle test for the steering part, we observed the parameters: steering torque and variation of length for the actuator when it turns left and right. The observed results are compared and analyzed by the simulation and vehicle test experiment.

Finally, we designed and developed the tire roller prototype on the basis of this simulation.

REFERENCES

[1] J. B. Song and S. M. Lee, "Engine torque and engine/automatic transmission speed control systems using time delay control," *Journal of Control, Automation and Systems Engineering*, vol. 2, no. 2, pp. 81-87, June 1996.

[2] J. H. Kim, *Hydraulic System Design and Vehicle Dynamic Modeling for the Construction Equipment*, Master's Thesis, Kookmin University, Seoul, Korea, 2001.

[3] C. S. Park, *A Research and Analysis about Development of Hydraulic Circuit System of Hydrostatic Tire Roller*, Master's Thesis, Kookmin University, Seoul, Korea, 2001.

[4] J. R. Ellis, *Vehicle Handling Dynamics*, Mechanical Engineering Publications Limited, London, 1994.

[5] Y. J. Cho, S. H. Ha, K. S. Yi, and S. J. Heo, "Modeling and control of a hydraulic brake actuator for vehicle collision avoidance systems," *Journal of Control, Automation and Systems Engineering*, vol. 6, no. 7, pp. 537-543, July 2000.
[6] J. A. Sullivan, *Fluid Power*, Prentice-Hall International Inc., 1998.
[7] H. E. Meritt, *Hydraulic Control Systems*, John Wiley & Sons Inc., 1967.
[8] G. H. Lee, *A Study on the Speed Control of a Closed-Loop Hydrostatic Transmission*, Ph.D. Dissertation, Seoul National University, Seoul, Korea, 1995.
[9] T. D. Gillespie, *Fundamentals of Vehicle Dynamics*, SAE, 1992.
[10] P. Grant, J. S. Freeman, R. Vail, and F. Huck, "Preparation of a virtual proving ground for construction equipment simulation," *Proc. of DETC'98, ASME Design Engineering Technical Conferences*, pp. 13-16, 1998.
[11] L. I. Buzdugan, O. Balling, P. C. Lee, C. Balling, J. S. Freeman, and F. Huck, "Multirate integration for real-time simulation of wheel loader hydraulic," *Proc. of DETC'99, ASME Design Engineering Technical Conferences*, pp. 12-15, 1999.
[12] S. G. Kim and J. H. Kim, "Modeling and validation of hydraulic system control for the construction equipment," *Proc. of the Modeling, Identification and Control, IASTED*, vol. 2, pp. 607-612, 2001.
[13] N. Instruments, *Lab-View Data Acquisition Basics Manual*, National Instruments, 1996.

Sang-Gyum Kim received the B.S. and M.S. degrees in Automotive Engineering from Kookmin University, Korea in 1996 and 1998, respectively. His main research interests are in the areas of unmanned vehicle systems, sensor fusion, vision process, hydraulic & control systems and system identification.

Jung-Ha Kim received the B.S. in 1981 from the Sung Kyun Kwan University in Korea, the M.S in 1986 from the University of Cincinnati, U.S.A., and the Ph.D. in 1990 from the University of Pennsylvania, U.S.A., all in Mechanical Engineering. His areas of interest includes unmanned vehicles, hydraulic systems, sensors, robotic & electronic control and system identification.

Woon-Sung Lee received the B.S. in Mechanical Design and Production Engineering from Seoul National University, Korea in 1978. He received the M.S. and Ph.D. degrees in Mechanical Engineering from the University of Iowa, U.S.A., in 1983 and 1987, respectively. His research interests include driving simulators, hardware-in-the-loop simulation, vehicle integrated control, 3D graphics and virtual reality.